Article

Thermal Performance of Concrete with Reactive Magnesium Oxide as an Alternative Binder

Javier A. Forero [1,2], Miguel Bravo [2,*], João Pacheco [2], Jorge de Brito [2] and Luís Evangelista [3]

1   Postgraduate Program in Structural Engineering and Construction (PECC),
    Predio SG-12 Campus Darcy Ribeiro, University of Brasília, Brasilia 70910-900, Brazil;
    javier.valencia@tecnico.ulisboa.pt
2   CERIS, Instituto Superior Técnico, Universidade de Lisboa, 1049-001 Lisbon, Portugal;
    joaonpacheco@tecnico.ulisboa.pt (J.P.); jb@civil.ist.utl.pt (J.d.B.)
3   CERIS, Instituto Superior de Engenharia de Lisboa, 1950-062 Lisbon, Portugal; evangelista@dec.isel.ipl.pt
*   Correspondence: miguelnbravo@tecnico.ulisboa.pt

Abstract: This study evaluates the thermal conductivity of concrete produced with reactive magnesium oxide (MgO) as a partial replacement for cement. MgO is a viable option for the concrete industry, mainly due to its benefits in sustainability and reducing CO_2 emissions compared to cement emissions. Four different MgO's produced in Australia, Canada, and Spain were used in concrete mixes as a partial replacement of cement at 5%, 10%, and 20% by mass. The experimental results showed that the thermal conductivity is higher when MgO increases in mixes after 28 days of curing. With the incorporation of MgO, the thermal conductivity increased between 3.2% and 10.2%, and the mechanical properties declined: compressive strength between 12.7% to 26.2%, splitting tensile strength between 9.7% to 34.0%, and modulus of elasticity between −4.1% to 7.8%. Finally, it is important to highlight that the addition of different contents of MgO in the concrete mixes modified the microstructure of the cement matrix. As a result, there was an increase in porosity, which negatively influenced the mechanical properties and thermal conductivity. Therefore, the relationships between these properties were also analyzed.

Keywords: reactive magnesium oxide; thermal conductivity; alternative binder; concrete

1. Introduction

The fast rise of global temperature following the onset of the industrial age has concerned many governments worldwide. Policies such as the Paris Agreement define targets for global temperature rise (1.5 °C in the case of the Paris agreement) [1]. This represents a major challenge for industrial sectors such as the construction industry, which releases 11% of all carbon dioxide (CO_2) into the atmosphere per year [2,3]. The cement industry alone was responsible for around 5.7 billion tonnes of CO_2 emissions in 2018 [4]. This led to the use of supplementary cementitious materials with lower CO_2 emissions. A promising alternative solution is using reactive magnesium oxide (MgO) as a supplementary cementitious material. This binder can absorb CO_2 in stable carbonates during hydration [5]. Despite non-reactive MgO being already used in refractory cement [6], standards restrict MgO content in cement to a maximum of 5% [7].

The production of reactive MgO by calcination of the extracted magnesite ($MgCO_3$) occurs at temperatures between 700 °C and 1000 °C in an endothermic reaction, as presented in Equation (1). This low calcination temperature used for the production of reactive MgO compared to the production of Portland cement (between 700 °C and 2800 °C) allows the use of alternative fuels with lower heating values [8]. The ideal temperature for the calcination of $MgCO_3$ depends on several aspects, such as impurities content and physical properties of the raw material. However, increasing temperatures in the calcination of $MgCO_3$ produce changes in the crystalline structure, reducing its reactivity by reducing

its specific surface area and increasing the particle size [9–12]. The calcination of $MgCO_3$ also determines the classification of the MgOs produced on the market. According to the European Commission, MgO grades are defined as caustic calcined (the case of reactive MgO), 600–1300 °C; dead burnt, 1600–2200 °C; and fused, >2800 °C [13].

$$MgCO_3 \rightarrow MgO + CO_2 \tag{1}$$

The hydration of MgO happens rapidly when the anhydrous surface of MgO comes into contact with water to form a surface layer of Mg (OH)$_2$ (Equation (2)), limited by the rate at which Mg++ and OH- ions, both dissolved, are removed from the water layer. MgO also reacts with CO_2 in the presence of water to produce hydrated carbonates or hydroxy-carbonates (Equation (3)) such as nesquonite ($MgCO_3 3H_2O$) [14–16]. The formation of Mg (OH)$_2$ produces an expansion in the matrix of the binder explained by the pressure of crystal growth Mg (OH)$_2$ or the expansion pressure due to the growth of Mg (OH)$_2$. This expansive nature can be controlled by the reactivity and fineness of the MgO used. The higher the calcination temperature of MgO, the less expansion in the early ages and the longer the hydration process lasts. Experiments that studied the incorporation of reactive MgO as a binder in cementitious matrices have shown that there is a reduction in the mechanical properties such as compressive strength [16–26], flexural strength [17–22], and splitting tensile strength [22,23].

$$MgO + H_2O \rightarrow Mg (OH)_2 \tag{2}$$

$$Mg (OH)_2 + CO_2 + 2H_2 0 \rightarrow MgCO_3.3H_2 0 \tag{3}$$

Authors such as Mavroulidou et al. [24] showed a reduction in compressive strength in ternary concrete mixes with fly ash (FA), metakaolin, and reactive MgO. This reduction is proportional to the increase of MgO content, around 30%. While the water/binder (w/b) ratio was kept constant (0.55) for all mixes presented in Mavroulidou et al. [24], these authors reported this reduction and mentioned that MgO increased the porosity and the production of magnesium silicate hydrates. This occurred because FA and brucite did not react to form the M-S-H gel.

Unluer and Al-Tabbaa [25] studied the compressive strength under accelerated carbonation of 10% CO_2 in concrete blocks with reactive MgO and with or without pulverized fuel ash (PFA). The mixes with MgO and PFA showed strength developments with values reaching 10.6 MPa. On the other hand, the MgO mixes achieved a strength of 4.0 MPa after only 1 day of carbonation. Carbonation of the MgO and PFA blends led to 110% higher strengths than those of the MgO-only blends, which showed that the latter's lower densities provided relatively more porous structures available for strength development through the formation of hydrated magnesium carbonates (HMC). Mixes with a w/b ratio of 0.6 with one day of curing presented a low strength of around 4 MPa due to the delay of the hydration and carbonation processes, producing an HMC in less quantity. On the other hand, the relatively humid mixes with a w/c ratio of 0.9 saturated the pores with water, which hindered the transport of CO_2 through the samples and delayed the formation of HMC, leading to low strength results in the samples for the same curing periods (3 MPa for 7 days of curing).

The MgO-PFA mixes had strengths of up to 7.0 MPa and 17.4 MPa after 1 and 7 days of exposure to a CO_2 concentration of 5%, meeting the strength requirement for the blocks, 7 MPa. From 1 to 7 days, average increases in strength of 160%, 120%, and 70% were achieved in MgO-PFA mixes exposed to CO_2 concentrations of 5%, 10%, and 20%, respectively, showing that CO_2 concentration is not the limiting factor for complete carbonation of the MgO. A study by Gao et al. [19] observed that the parameters used for autoclave curing also influence the compressive strength, which increases with autoclave time and decreases with autoclave temperature increment. Summing up, the compressive strength values were higher in the mixes with 4% MgO, followed by those with 8% and 12%.

Reactive MgO also influences other mechanical properties, such as tensile strength and modulus of elasticity. Again, studies from Mavroulidou et al. [24] showed that the splitting tensile strength of concrete mixes produced with different contents of reactive MgO, FA, and metakaolin fell by less than 10% with the simultaneous incorporation of 10% MgO and 20% FA.

Regarding the modulus of elasticity, Choi et al. [26] explained the influence of incorporating MgO after freeze-thaw cycles in concrete mixes produced with 20% FA, and different w/b ratios of 0.48 and 0.65, cured in water for 28 days or 360 days. This incorporation led to a slight increase of 4% of the modulus of elasticity in concrete mixes after 100, 200, and 300 freeze-thaw cycles. This explains why reactive MgO mixes have an initial expansive nature and less shrinkage than concrete with conventional cement.

Thermal conductivity is a physical property that describes the ability to conduct heat in concrete elements [27]. A higher conductivity is due to higher density [28]. MgO is a material widely used by manufacturers of electrical resistors. Slifka et al. [29] validated their experimental thermal conductivity technique using MgO as it has a high thermal conductivity.

Vo et al. [30] studied concrete mixes with fly ash and MgO. They observed higher thermal conductivity in mixes with a lower content of fly ash (15%) and higher MgO content (7.5%) in comparison to those with higher content of FA and lower content of MgO. This phenomenon is explained by MgO having higher thermal conductivity than FA and cement. Ruan and Unluer [31] studied compositions made with cement with high MgO content. The thermal conductivity of the highest MgO cement samples after 7 days of curing showed an increase in thermal conductivity. This increase was associated with greater porosity in samples with higher water contents, leading to higher conductivity.

Based on this review, it can be concluded that the incorporation of MgO and its influence on the mechanical properties largely depend on the reactivity of MgO and the MgO content [12,22,32]. The MgO hydration reactions produce magnesium hydroxide, which leads to an increase in volume and reduces the shrinkage of concrete [33]. In summary, highly reactive MgO can present dimensional stability problems because expansion reactions can mitigate the shrinkage of cementitious matrices [34]. With respect to thermal conductivity, reactive MgO increases this property because MgO has higher thermal conductivity than cement [29,31,35].

This study analyses the influence of incorporating different MgOs produced in Australia, Canada, and Spain, with replacement contents of 5%, 10%, and 20% of cement by mass, on the mechanical properties and thermal conductivity. The detailed analysis of thermal performance done in this article fills a gap in state of the art concerning concrete with reactive magnesium oxide. In the literature, there is no study that evaluates the thermal behavior of concrete with different MgOs. In addition to thermal performance, compressive strength, splitting tensile strength, and modulus of elasticity tests were performed in this study to understand better the effect of reactive MgO in concrete. Correlations were made between mechanical properties and thermal properties to have a complete overview of the influence of MgO as a partial substitute for cement on thermal conductivity and specific thermal capacity. These correlations didn't exist in the literature.

## 2. Materials and Methods

2.1. Experimental Procedure

2.1.1. Materials

The main cementitious binder of the reference concrete (RC) was CEM I 42.5 R, manufactured by the Secil (Setúbal, Portugal) company. For all compositions, two types of natural aggregates were used: coarse aggregates with commercial classification in compliance with the designations 2/6, 6/12, and 12/20 and silica sands with the designations 0/2 and 0/4. These grading distributions are in accordance with EN 12620 [36].

The MgOs used in this research as a partial cement substitute were manufactured in three different countries, Australia, Canada, and Spain, each designated as A (Australia),

C (Canada), and S0 or S1 (Spain) and were calcined at temperatures between 700 °C and 1000 °C. The particle size of MgO was evaluated for the Spanish MgO to check its effect on reactivity. To reduce the particle size, a pre-treatment of MgO from Spain was carried out, which consisted in grinding for one hour in a rotary mill with steel balls of 2–4 cm diameter to ensure that a particle size distribution would be similar to cement. The distribution of this new particle size was named S1, while S0 is used to label the Spanish MgO that was used as supplied by the manufacturer. This pre-treatment was not analyzed for the MgOs from Australia and Canada since their particle size distribution is already similar to cement.

Figure 1a,b presents the specific surface (Figure 1a, purity; Figure 1a, reactivity; Figure 1b; and skeletal density, Figure 1b) of all MgOs used in this investigation. These results were obtained through X-ray fluorescence (XRF) and Brunauer-Emmett-Teller (BET) analysis and the reactivity test with acetic acid. The chemical composition of the solid raw materials was evaluated using a non-corrosive wavelength dispersive X-ray fluorescence spectrometry analysis (XRF), using a ZSX PRIMUS IV (Rigaku, Cordoba, Spain) equipment with a power of 4 kW. BET analysis has been carried out with the equipment Sievert PCT-Pro 2000 (Cordoba, Spain). The reactivity test measured the time duration required to neutralize an acidic solution (in this case, 0.25M acetic acid) by a certain MgO sample.

(**a**)

(**b**)
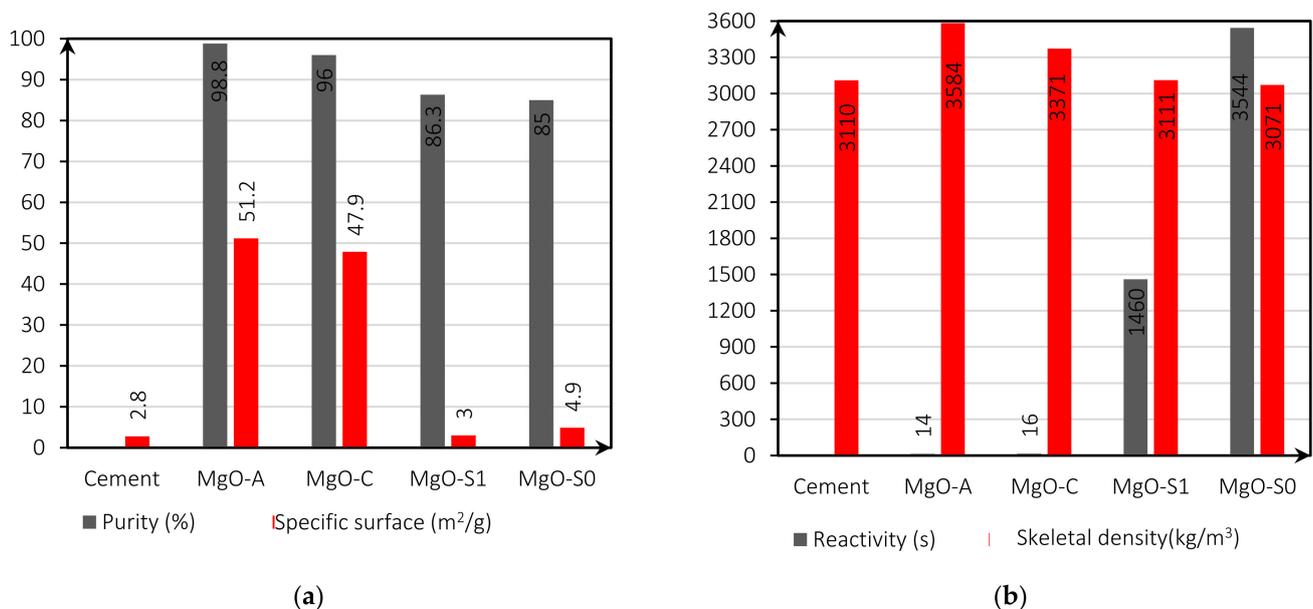
Figure 1. Characteristics of the various reactive MgO's and cement: purity (%) and specific surface (m^2/mg) (**a**); reactivity (s) and skeletal density (kg/m^3) (**b**).

The specific surface is an important factor since it directly determines the reactivity of MgO. Purity shows the contents of the elements that compose the MgO from each supplier. As shown in Figure 1a, the purity of the MgOs depends on the supplier: MgO-A has a high MgO content of 98.8%, while MgO-S0, MgO-S1, and MgO-C have a lower MgO content of 85%, 86.3%, and 96%, respectively. The main impurities are SiO_2, CaO, and Fe_2O_3. Regarding the density, all MgO has a skeletal density greater than 3000 (kg/m^3), namely MgO-A, with a value of 3584 (kg/m^3). The reactivity (s) of MgO-S0 and MgOS1 showed significantly higher values (lower reactivities) than MgO-A and MgO-C. This is because, on the one hand, the MgO-S0 particles have a very large dimension. On the other hand, the milling process left MgO-S1 with a more spherical shape (smaller specific surface).

2.1.2. Tests

Thermal conductivity testing was conducted on an ISOMET 2114 analyzer from Applied Precision Ltd. (Lisbon, Portugal). Two 100 × 100 × 500 mm prismatic specimens

of each mix cured at 28 days in a dry chamber (20 ± 2 °C, 50% RH) were analyzed in these tests, taking at least three readings per sample at a frequency between 0.2–2 W/m·K and 2–3 W/m·K.

The compressive strength was made in four hardened 150 × 150 × 150 mm cubic specimens according to EN 12390-3 [37]. The splitting tensile strength test was carried out on three cylindrical specimens of 150 × 300 mm, following the method presented in EN 12390-6 [38]. The secant modulus of elasticity test was carried out on two cylindrical specimens of 150 × 300 mm as described in LNEC E 397 [39]. All specimens for the compressive strength, tensile strength, and modulus of elasticity tests were cured for 28 days in a wet chamber before testing.

2.1.3. Mixing and Mix Design

The mixing of concrete was done in three stages. In the first one, the coarse aggregates were mixed with 2/3 of the total water for 4 min. In the second stage, the fine aggregates were added for 4 min. In the end, binders and 1/3 of water were added during the remaining time of the mixing procedure.

All compositions presented in this study were based on the methodology proposed by Nepomuceno et al. [40], attending to the following parameters: C30/37 strength class, XC3 exposure class, and S2 slump in accordance with the EN 206 standard [41]. The volume content of the materials is shown in Figure 2. All mixes were developed based on the reference composition with small changes in the solid volume to respect the different w/c ratios and maintain the target slump.
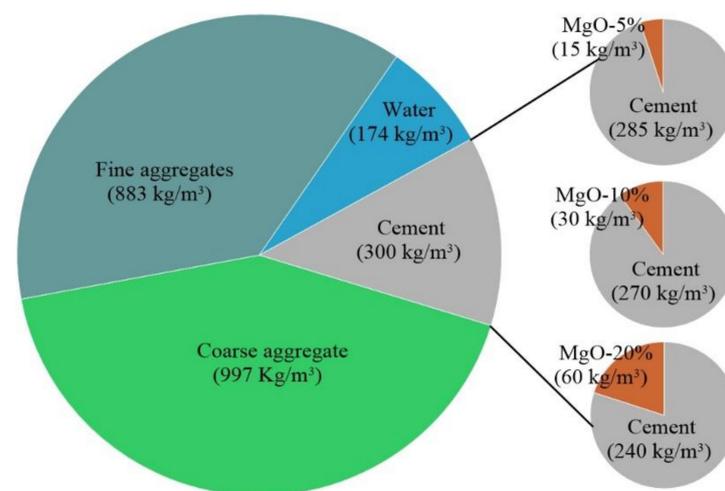

Figure 2. Composition of the reference concrete (RC).

The concrete composition has a great impact on the thermal conductivity and mechanical properties of concrete due to the formation of hydration products, which determine the number of pores associated with the cement matrix. This formation of hydration products (HMC) is directly associated with the amount of MgO in the mixes [30,42]. The replacement of cement with reactive MgO was made by mass at 5%, 10%, and 20%. The contents were defined in accordance with the results obtained by Bravo et al. [22]. These authors studied the mechanical behavior and durability of mortar made with the same reactive MgO used in our experiment. MgO was used as a partial replacement of cement at 0%, 5%, 10%, 15%, 20% and 25% by mass.

In this research work, the mixes were labeled according to the MgO source along with the percentage of cement replacement with reactive MgO. Concrete with partial replacement of reactive MgO from Spain, without crushing treatment, was called S0, concrete with reactive MgO and crushing treatment for one hour was called S1, and concretes with MgO from Australia and Canada were called A and C, respectively. To designate the proportion of incorporation of MgO in the mixes, a nomenclature that first designates the amount

of substitution and then the origin where it has been used was applied. For example, A5 describes a concrete mix with 5% MgO from Australia. Concrete without the addition of MgO was referred to as RC.

Another important factor to mention is the range of the fresh-state consistency. As seen in Figure 3b, all mixes are within the S2 slump range. For this purpose, it was necessary to increase the water/binder ratio in the mixes when the reactive MgO increased. Figure 3a shows that all mixes are within the S2 consistency range when the reactive MgO content increases.


(**a**)

(**b**)
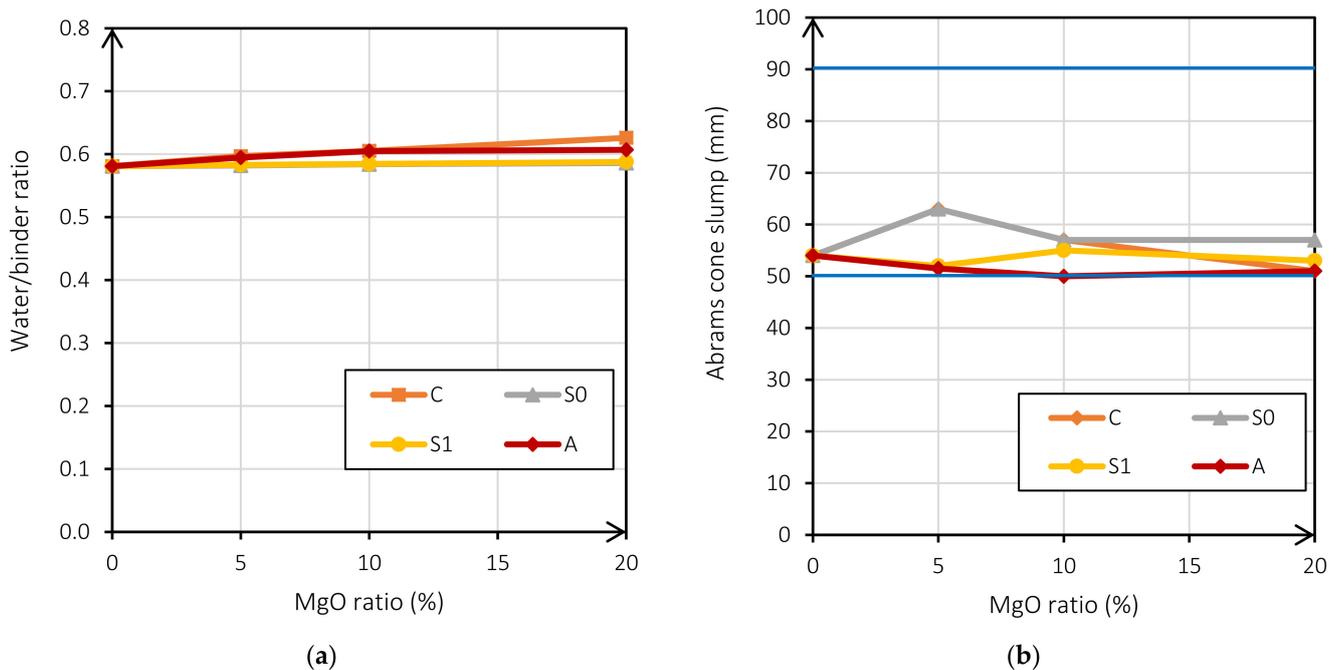
Figure 3. W/b ratio according to the MgO ratio (%) (**a**); Abrams cone slump (mm) according to the MgO ratio (%) (**b**).

3. Experimental Results and Discussion

Figure 4 shows the average compressive strength values, splitting tensile strength and modulus of elasticity of all compositions related to RC. As the MgO content increased, the compressive strength decreased related to RC. The C5-MgO result is the average value of the compressive strength of compositions C5-A, C5-C, C5-S, and C5-S0 with a value of 44.5 MPa. This 12.7% reduction in compressive strength can be explained by two phenomena during hydration. The first is associated with the fact that, with an increase in the MgO content, the C2S and C3S products decrease, and consequently, the formation of CSH is lower, increasing the formation of a less resistant product Mg $(OH)_2$ [18,43,44]. The second reason is associated with MgO expansion, increasing micro-cracking, resulting in an increase in porosity and macropores, which directly influences compressive strength [45,46]. The same behavior was found by Choi et al. [26], who observed reductions between 5% and 13% for curing ages of 7 to 28 days in mixes incorporating 5% MgO and 20% FA. The mean values for C10-MgO and C20-MgO were 42.0 MPa and 37.6 MPa, respectively.

The average splitting tensile strength of the mixes showed reductions of 9.7%, 20.1%, and 34.0% for C5-MgO, C10-MgO, and C20-MgO, respectively. One of the factors that can explain this phenomenon in addition to the above is that, for blends A and C, the w/b ratio was slightly higher, increasing the production of pores, in addition to the fact that S1 blends had a grinding pre-treatment, decreasing the surface area of the particle and preventing the complete hydration of the MgO particles. This decrease in MgO surface area was due to the rounding of the particles when using this milling process. The same trend was observed by

Mavroulidou et al. [24], who had 10% reductions in splitting tensile strength with reactive MgO in binary mixes of fuel ash and metakaolin.
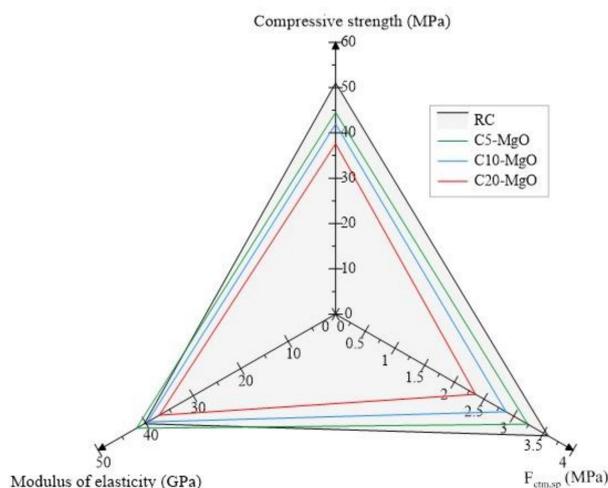
Figure 4. Main mechanical properties.

In contrast to the compressive strength and splitting tensile strength trends, there is an increase in the modulus of elasticity values for the concrete mix with 5% MgO. This slight increase (4.1%) can be explained due to the expansive nature of MgO, which increases bulk density and decreases shrinkage [12,32,47–49]. The mean values of the C5-MgO, C10-MgO, and C20-MgO mixes were 42.0 GPa, 39.7 GPa, and 37.2 GPa, respectively.
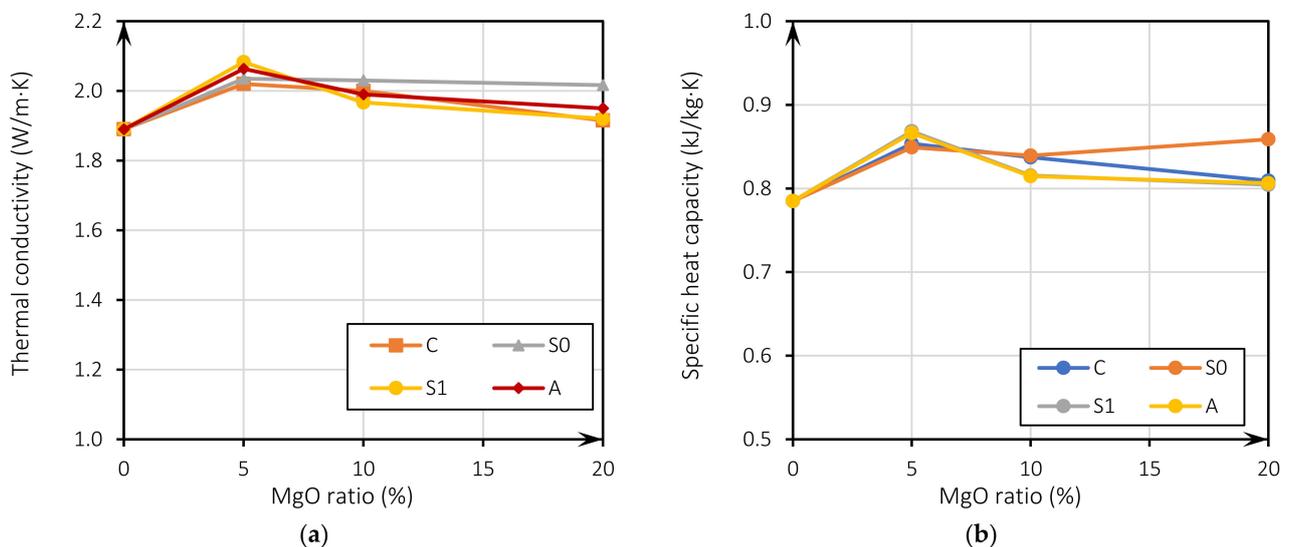
4. Thermal Conductivity

Table 1 lists the values of thermal conductivity and specific heat capacity as well as their standard deviations for each MgO incorporation ratio of the different mixes at 28 days of curing in a wet chamber. It shows an increase in thermal conductivity (λ) between 6.9% to 10.2% (5% incorporation of MgO), 4.1% to 7.4% (10% incorporation of MgO), and 1.3% to 6.7% (20% incorporation of MgO). This increase in conductivity is because MgO is considered a highly thermally conductive material [29]. The higher amount of MgO incorporation reduces the amount of HSC produced and increases the production of Mg $(OH)_2$, thus increasing the thermal conductivity [29,30,50,51]. Vo et al. [30] studied the effect of binary mixes of reactive magnesium oxide and fly ash in concrete, increasing thermal conductivity with the increase of MgO and decrease of fly ash. Vo et al. [30] reported that this effect is due to the filling and hydration of fly ash and the thermal nature of MgO particles.

Figure 5a shows the evolution of thermal conductivity related to the incorporation of MgO for all mixes. It can be observed that there is an increase in the value of the thermal conductivity for 5% of MgO incorporation in all the mixes regarding the RC. It is noteworthy that the increase in thermal conductivity is greater until a 10% substitution ratio, being less noticeable for 20% substitutions (between 1.6% and 6.7%). There is a clear loss of thermal conductivity for the MgOs of Australia, Canada, and Spain (S1), with the increase of the incorporation to 10% and 20%. The thermal conductivity tends to be higher in mixes where the w/b ratio is closer to RC. This can be seen in the results shown in Figure 3, and was associated with the higher porosity of the samples with higher water content, leading to a lower thermal conductivity [31,52–54]. This may also mean that the thermal effect of MgO is more effective in mixes with lower w/b ratios. As the variation of the thermal conductivity is similar for all analyzed MgOs, it is considered that this improvement is due to the thermal properties of the MgOs not being significantly affected by the different physical characteristics of the different analyzed MgO.

Table 1. Thermal properties of the concrete mix results at 28 days.

Mix	Thermal Conductivity (W/m·K)			Specific Heat Capacity (kJ/kg·K)	
	28	**σ**	**ΔRC**	**28**	**ΔRC**
RC	**1.89**	**0.2**	**-**	**0.78**	**-**
C5:C	2.02	0.1	6.9%	0.85	8.7%
C10:C	2.00	0.0	5.8%	0.84	6.7%
C20:C	1.92	0.1	1.3%	0.81	3.1%
C5:S0	2.04	0.0	7.7%	0.85	8.2%
C10:S0	2.03	0.1	7.4%	0.84	6.9%
C20:S0	2.02	0.1	6.7%	0.86	9.4%
C5:S1	2.08	0.1	10.2%	0.87	10.6%
C10:S1	1.97	0.0	4.1%	0.82	3.9%
C20:S1	1.92	0.1	1.6%	0.80	2.5%
C5:A	2.06	0.0	9.2%	0.87	10.4%
C10:A	1.99	0.1	5.3%	0.81	3.8%
C20:A	1.95	0.1	3.2%	0.81	2.7%

Figure 5. Thermal conductivity versus MgO incorporation ratio (**a**); specific heat capacity versus MgO incorporation ratio (**b**).

The specific heat capacity (kJ/kg·K) was calculated as per Equation (4), where c_p is the volumetric heat capacity in J/m^3K, and dry corresponds to the dry density of concrete in kg/m^3. Results are shown in Figure 5b, where the specific heat value is observed, as well as its improvement with respect to RC. Figure 5b displays the evolution of the specific heat capacity as a function of the MgO incorporation ratio for all mixes. As previously described, the specific heat capacity follows the same trend as thermal conductivity. All the values lie within a normal range (0.790 kJ/m^3·K to 0.960 kJ/m^3·K) for concrete, used in residential building construction [55]. Furthermore, thermal conductivity of concrete with MgO is higher or is within the range recommended by Eurocode 2 [56]: 1.95 W/m·K to 1.33 W/m·K.

$$C_p = \frac{c}{\rho_{dry}} \tag{4}$$

5. Relationships between Thermal Properties and Mechanical Properties

Figure 6a shows the relationship between thermal conductivity and dry density. The thermal conductivity is higher for mixes with MgO content of 5%. This is because the w/b ratio is lower, producing fewer pores (Figure 6b) [5]. Figure 6c presents thermal conductivity as a function of the compressive strength for all mixes. Figure 6c shows that

the thermal conductivity of the mixes with MgO from Australia, Canada, and Spain without treatment is linearly related to the compressive strength with an R^2 of 0.91, 0.89, and 0.96, respectively. This relationship is linked to the expansive nature of MgO. Reactive MgO can cause cracking and thus lead to increased porosity and macropores, a determining factor in strength and thermal conductivity [5,45]. This indicates that the lower the compressive strength, the higher the thermal conductivity. On the other hand, mixes with MgO from Spain with treatment showed an R^2 coefficient of 0.65, indicating a weak relationship between these properties. Vo et al. [30], in their investigation on concretes with MgO and fly ash, also found this same trend. The higher the MgO content incorporated in the mix, the lower the compressive strength and the higher the thermal conductivity. Moreover, the specific heat capacity is also correlated with compressive strength. Figure 6c presents this correlation showing an R^2 between 0.65 and 0.97, with a weak correlation of $R^2 = 0.65$ for the mixes with the MgO from Spain (S1), and a strong correlation for the mixes with MgO from Spain without treatment R^2 of 0.96 and Australia R^2 of 0.91.
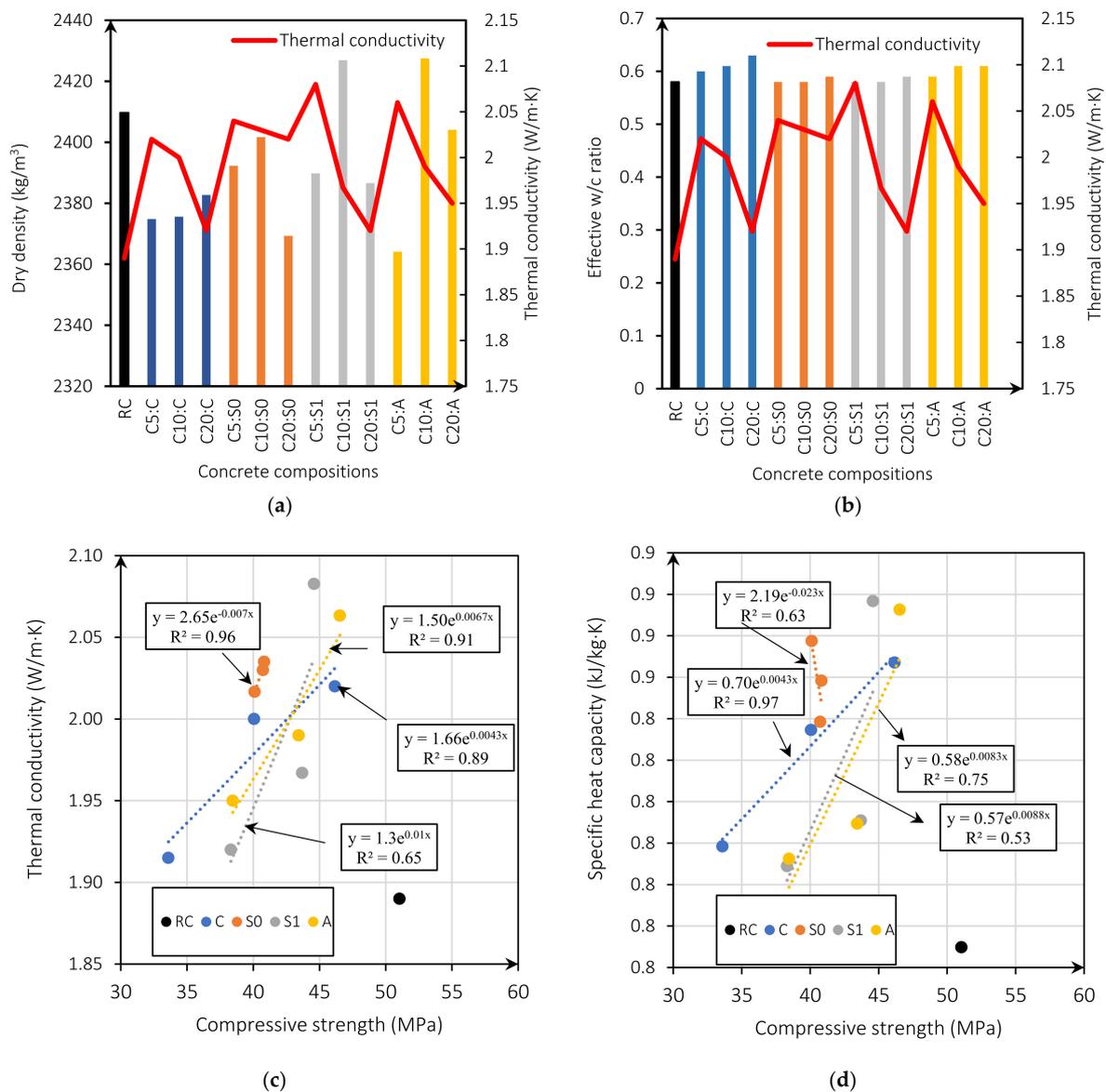
Figure 6. Thermal conductivity (W/m·K) versus dry density (kg/m^3) (**a**); thermal conductivity (W/m·K) versus effective w/b ratio (**b**); compressive strength versus thermal conductivity (W/m·K) (**c**); and compressive strength versus specific heat capacity (kJ/kg·K) (**d**).

6. Conclusions

This work advocates the replacement of part of the cement with reactive MgO as a solution to reduce CO_2 emissions without much damage to the mechanical properties and the thermal conductivity. This study presented the results of MgOs derived from several countries. The treatment of MgO from Spain shows that mixes with MgO S1 present worse results in all properties. This refers to the milling of MgO-S that reduces the surface area of the particle size, limiting the complete hydration of the MgO particles. Properties such as compressive strength and splitting tensile strength, when MgO is incorporated in the mix, do not show a significant reduction in relation to RC.

Regarding thermal conductivity, the mixes made with MgO showed a higher thermal conductivity than RC. As was discussed, this result depends on the thermal properties of MgO, which has a higher electrical conductivity. As the variation of the thermal conductivity is similar for all analyzed MgOs, it is considered that this increase is due to the thermal properties of the MgOs not being significantly affected by the different physical characteristics of the different analyzed MgO. Specific heat capacity followed the same trend. This similar trend confirms previous studies by other authors that describe mixes using only cement. Thermal conductivity can describe the temperature distribution within the concrete structural elements. When analyzing the thermal behavior of concrete with MgO incorporation, it can be concluded that the thermal behavior of these mixes will increase this distribution. All the mixes with MgO were worse than or within the range defined by Eurocode 2 [56].

The concrete mixes with higher w/b ratios presented a lower conductivity than those with lower w/b. As explained, this phenomenon proves there is a decrease in the thermal effect of MgO in mixes with higher w/b ratios.

Finally, the correlations of mechanical properties and thermal conductivity establish necessary parameters to determine the influence of MgO hydration and its thermal conductivity, which is necessary for building design.

References

1. Schleussner, C.-F.; Rogelj, J.; Schaeffer, M.; Lissner, T.; Licker, R.; Fischer, E.M.; Knutti, R.; Levermann, A.; Frieler, K.; Hare, W. Science and policy characteristics of the Paris Agreement temperature goal. *Nat. Clim. Chang.* **2016**, *6*, 827–835. [CrossRef]
2. Nilsson, A.; Hans, F.; Lopez Legarreta, P.; Lui, S.; Röser, F. *Decarbonisation Pathways for the EU Cement Sector*; Technology Routes and Potential Ways Forward; NewClimate Institute: Berlin, Germany, 2020.
3. Dean, B.; Dulac, J.; Petrichenko, K.; Graham, P. *Global Status Report 2016: Towards Zero-Emission Efficient and Resilient Buildings*; UN Environment Programme: Nairobi, Kenya, 2016.
4. Andrew, R.M. Global CO_2 emissions from cement production. *Earth Syst. Sci. Data* **2018**, *10*, 195–217. [CrossRef]
5. Unluer, C.; Al-Tabbaa, A. Enhancing the carbonation of MgO cement porous blocks through improved curing conditions. *Cem. Concr. Res.* **2014**, *59*, 55–65. [CrossRef]
6. Amaral, L.; Oliveira, I.; Salomão, R.; Frollini, E.; Pandolfelli, V. Temperature and common-ion effect on magnesium oxide (MgO) hydration. *Ceram. Int.* **2010**, *36*, 1047–1054. [CrossRef]
7. *EN 197-1:2011*; Cement–Part 1: Composition, Specifications and Conformity Criteria for Common Cements. British Standards Institution: London, UK, 2000.

8. Ruan, S.; Unluer, C. Comparative life cycle assessment of reactive MgO and Portland cement production. *J. Clean. Prod.* **2016**, *137*, 258–273. [CrossRef]

9. Shand, M.A. *The Chemistry and Technology of Magnesia*; John Wiley & Sons: Hoboken, NJ, USA, 2006.

10. Canterford, J. Magnesia—An important industrial mineral: A review of processing options and uses. *Miner. Process. Extr. Metall. Rev.* **1985**, *2*, 57–104. [CrossRef]

11. Green, J. Calcination of precipitated Mg (OH) 2 to active MgO in the production of refractory and chemical grade MgO. *J. Mater. Sci.* **1983**, *18*, 637–651. [CrossRef]

12. Nobre, J.; Ahmed, H.; Bravo, M.; Evangelista, L.; de Brito, J. Magnesia (MgO) Production and Characterization, and Its Influence on the Performance of Cementitious Materials: A Review. *Materials* **2020**, *13*, 4752. [CrossRef]

13. Schorcht, F.; Kourti, I.; Scalet, B.M.; Roudier, S.; Sancho, L.D. *Best Available Techniques (BAT) Reference Document for the Production of Cement, Lime and Magnesium Oxide*; European Commission Joint Research Centre Institute for Prospective Technological Studies: Luxembourg, 2013.

14. Mo, L.; Deng, M.; Tang, M.; Al-Tabbaa, A. MgO expansive cement and concrete in China: Past, present and future. *Cem. Concr. Res.* **2014**, *57*, 1–12. [CrossRef]

15. Zhang, S.; Lee, W. Spinel-containing refractories. In *Refractories Handbook*; CRC Press: Boca Raton, FL, USA, 2004; Volume 178, p. 215.

16. Walling, S.A.; Provis, J.L. Magnesia-based cements: A journey of 150 years, and cements for the future? *Chem. Rev.* **2016**, *116*, 4170–4204. [CrossRef]

17. Mo, L.; Liu, M.; Al-Tabbaa, A.; Deng, M.; Lau, W.Y. Deformation and mechanical properties of quaternary blended cements containing ground granulated blast furnace slag, fly ash and magnesia. *Cem. Concr. Res* **2015**, *71*, 7–13. [CrossRef]

18. Mo, L.; Liu, M.; Al-Tabbaa, A.; Deng, M. Deformation and mechanical properties of the expansive cements produced by inter-grinding cement clinker and MgOs with various reactivities. *Constr. Build. Mater.* **2015**, *80*, 1–8. [CrossRef]

19. Gao, P.-W.; Wu, S.-X.; Lu, X.-L.; Deng, M.; Lin, P.-H.; Wu, Z.-R.; Tang, M.-S. Soundness evaluation of concrete with MgO. *Constr. Build. Mater.* **2007**, *21*, 132–138. [CrossRef]

20. Moradpour, R.; Taheri-Nassaj, E.; Parhizkar, T.; Ghodsian, M. The effects of nanoscale expansive agents on the mechanical properties of non-shrink cement-based composites: The influence of nano-MgO addition. *Compos. Part B Eng.* **2013**, *55*, 193–202. [CrossRef]

21. Lau, W.Y. The Role of Reactive MgO as an Expansive Additive in the Shrinkage Reduction of Concrete. Ph.D. Thesis, University of Cambridge, Cambridge, UK, 2019.

22. Bravo, M.; Forero, J.A.; Nobre, J.; De Brito, J.; Evangelista, L. Performance of Mortars with Commercially-Available Reactive Magnesium Oxide as Alternative Binder. *Materials* **2021**, *14*, 938. [CrossRef]

23. Pu, L.; Unluer, C. Investigation of carbonation depth and its influence on the performance and microstructure of MgO cement and PC mixes. *Constr. Build. Mater.* **2016**, *120*, 349–363. [CrossRef]

24. Mavroulidou, M.; Morrison, T.; Unsworth, C.; Gunn, M. Properties of concrete made of multicomponent mixes of low-energy demanding binders. *Constr. Build. Mater.* **2015**, *101*, 1122–1141. [CrossRef]

25. Unluer, C.; Al-Tabbaa, A. Impact of hydrated magnesium carbonate additives on the carbonation of reactive MgO cements. *Cem. Concr. Res* **2013**, *54*, 87–97. [CrossRef]

26. Choi, S.-W.; Jang, B.-S.; Kim, J.-H.; Lee, K.-M. Durability characteristics of fly ash concrete containing lightly-burnt MgO. *Constr. Build. Mater.* **2014**, *58*, 77–84. [CrossRef]

27. Bhattacharjee, B.; Krishnamoorthy, S. Permeable porosity and thermal conductivity of construction materials. *J. Mater. Civ. Eng.* **2004**, *16*, 322–330. [CrossRef]

28. Nguyen, H.-A.; Chang, T.-P.; Shih, J.-Y.; Chen, C.-T.; Nguyen, T.-D. Engineering properties and durability of high-strength self-compacting concrete with no-cement SFC binder. *Constr. Build. Mater.* **2016**, *106*, 670–677. [CrossRef]

29. Slifka, A.J.; Filla, B.J.; Phelps, J. Thermal conductivity of magnesium oxide from absolute, steady-state measurements. *J. Res. Natl. Inst. Stand. Technol.* **1998**, *103*, 357. [CrossRef] [PubMed]

30. Vo, D.-H.; Hwang, C.-L.; Tran Thi, K.-D.; Yehualaw, M.D.; Chen, W.-C. Effect of fly ash and reactive MgO on the engineering properties and durability of high-performance concrete produced with alkali-activated slag and recycled aggregate. *J. Mater. Civ. Eng.* **2020**, *32*, 04020332. [CrossRef]

31. Ruan, S.; Unluer, C. Influence of mix design on the carbonation, mechanical properties and microstructure of reactive MgO cement-based concrete. *Cem. Concr. Compos.* **2017**, *80*, 104–114. [CrossRef]

32. Forero, J.A.; Bravo, M.; Pacheco, J.; de Brito, J.; Evangelista, L. Fracture Behaviour of Concrete with Reactive Magnesium Oxide as Alternative Binder. *Appl. Sci.* **2021**, *11*, 2891. [CrossRef]

33. Rehsi, S. Magnesium oxide in portland cement. In *Advances in Cement Technology*; Elsevier: Amsterdam, The Netherlands, 1983; pp. 467–483.

34. Gonçalves, T.; Silva, R.; De Brito, J.; Fernández, J.; Esquinas, A. Hydration of reactive MgO as partial cement replacement and its influence on the macroperformance of cementitious mortars. *Adv. Mater. Sci. Eng.* **2019**, *2019*, 9271507. [CrossRef]

35. Chau, C.K.; Li, Z. Accelerated reactivity assessment of light burnt magnesium oxide. *J. Am. Ceram. Soc.* **2008**, *91*, 1640–1645. [CrossRef]

36. *BS EN 12620:2002*; Aggregates for Concrete. British Standards Institution: London, UK, 2002.

37. *EN 12390-3:2019*; Testing Hardened Concrete—Part 3: Compressive Strength of Test Specimens. European Committee for Standardization (CEN): Brussels, Belgium, 2009.

38. *BS EN 12390-6:2009*; Testing Hardened Concrete. Tensile Splitting Strength of Test Specimens. British Standards Institution: London, UK, 2009.

39. LNEC. *397-"Betões: Determinação do Módulo de Elasticidade em Compressão"*; Laboratório Nacional de Engenharia Civil: Lisbon, Portugal, 1993.

40. Nepomuceno, M.; Oliveira, L.; Lopes, S.M.R. Methodology for mix design of the mortar phase of self-compacting concrete using different mineral additions in binary blends of powders. *Constr. Build. Mater.* **2012**, *26*, 317–326. [CrossRef]

41. *BS EN 206:2013+A1:2016*; Concrete—Specification, Performance, Production and Conformity. British Standards Institution: London, UK, 2016; p. 98.

42. Vo, D.-H.; Hwang, C.-L.; Yehualaw, M.D.; Liao, M.-C. The influence of MgO addition on the performance of alkali-activated materials with slag–rice husk ash blending. *J. Build. Eng.* **2021**, *33*, 101605. [CrossRef]

43. Gonçalves, T.; Silva, R.; de Brito, J.; Fernández, J.; Esquinas, A. Mechanical and durability performance of mortars with fine recycled concrete aggregates and reactive magnesium oxide as partial cement replacement. *Cem. Concr. Compos.* **2020**, *105*, 103420. [CrossRef]

44. Vandeperre, L.; Liska, M.; Al-Tabbaa, A. Microstructures of reactive magnesia cement blends. *Cem. Concr. Compos.* **2008**, *30*, 706–714. [CrossRef]

45. Zheng, L.; Xuehua, C.; Mingshu, T. MgO-type delayed expansive cement. *Cem. Concr. Res.* **1991**, *21*, 1049–1057. [CrossRef]

46. Jang, J.-K.; Kim, H.-G.; Kim, J.-H.; Ryou, J.-S. The evaluation of damage effects on MgO added concrete with slag cement exposed to calcium chloride deicing salt. *Materials* **2018**, *11*, 793. [CrossRef] [PubMed]

47. Du, C. A review of magnesium oxide in concrete. *Concr. Int.* **2005**, *27*, 45–50.

48. Zhang, R.; Panesar, D.K. Mechanical properties and rapid chloride permeability of carbonated concrete containing reactive MgO. *Constr. Build. Mater.* **2018**, *172*, 77–85. [CrossRef]

49. Meddah, M.S.; Suzuki, M.; Sato, R. Influence of a combination of expansive and shrinkage-reducing admixture on autogenous deformation and self-stress of silica fume high-performance concrete. *Constr. Build. Mater.* **2011**, *25*, 239–250. [CrossRef]

50. Janowska, G.; Kucharska-Jastrzabek, A.; Kasiczak, A.; Rzymski, W. Thermal properties and combustibility of cross-linked XNBR/CSM blends: Part I. Influence of the magnesium oxide. *J. Therm. Anal. Calorim.* **2011**, *104*, 1107–1115. [CrossRef]

51. Yildirim, S.; Röcker, B. Active packaging. In *Nanomaterials for Food Packaging*; Elsevier: Amsterdam, The Netherlands, 2018; pp. 173–202.

52. Wong, J.M.; Glasser, F.; Imbabi, M. Evaluation of thermal conductivity in air permeable concrete for dynamic breathing wall construction. *Cem. Concr. Compos.* **2007**, *29*, 647–655. [CrossRef]

53. Collet, F.; Pretot, S. Thermal conductivity of hemp concretes: Variation with formulation, density and water content. *Constr. Build. Mater.* **2014**, *65*, 612–619. [CrossRef]

54. Ramos, M.O.; Pinheiro, I.G.; de Sousa Junior, L.G. Influência da porosidade na condutividade térmica, resistência mecânica e coeficiente de permeabilidade do concreto permeável. *Rev. Ibero-Am. Ciências Ambient.* **2021**, *12*, 515–528. [CrossRef]

55. Zhu, L.; Dai, J.; Bai, G.; Zhang, F. Study on thermal properties of recycled aggregate concrete and recycled concrete blocks. *Constr. Build. Mater.* **2015**, *94*, 620–628. [CrossRef]

56. *EN 1992-1-1:2004/A1:2014*; Eurocode 2: Design of Concrete Structures—Part 1-1: General Rules and Rules for Buildings. European Committee for Standardization: Brussels, Belgium, 2004.